

# WIRL Building Research Report

WOOD INNOVATION RESEARCH LABORATORY

**UNBC** UNIVERSITY OF  
NORTHERN BRITISH COLUMBIA  
**Wood Innovation  
Research Laboratory**

# Introduction

The purpose of this research is to investigate what differences, if any, exist between the modeled energy consumption and building envelope performance of the Wood Innovation Research Laboratory (WIRL) building following eight months of in-situ data collection. The WIRL building was completed in July of 2018 by the University of Northern British Columbia (UNBC) and is located in Prince George, British Columbia. Built in partnership with the Province of British Columbia, the building was designed to meet Passive House standards, a building certification system that requires the building to have low energy input requirements due to high levels of thermal insulation and minimal air leakage. To ensure the building achieves the established energy use targets set forth under the Passive House certification system, a computer model of the proposed building design must be completed prior to the start of construction using the Passive House Planning Package (PHPP) software. Inputs to the model include envelope design, mechanical energy use, building location and airtightness value. Key outputs included the predicted annual heating demand (kWh/m<sup>2</sup>a), total primary energy demand (kWh/m<sup>2</sup>a), and air tightness of the building envelope (ACH@50Pa).

Based on the final building design model and test results achieved following completion, the WIRL building was deemed to have met all Passive House requirements and certification was achieved.

To complete on-going data collection of the in-situ performance of the WIRL building, temperature and humidity sensors were installed in two of the exterior wall assemblies and the building's floor. In addition, gas and electrical energy use meters were installed to monitor the building's energy consumption. The installation of all equipment was made possible by Forest Innovation Investment through their 2018/2019 Wood First Program.

# Background

## University of Northern British Columbia

Located in the spectacular landscape of Northern B.C., home to the heart of the British Columbia forestry industry, the University of Northern British Columbia (UNBC) is one of Canada's best small universities. Rated #2 in the Primarily Undergraduate category of Maclean's magazine's 2019 university rankings, UNBC has been in the top three for the last 11 years. UNBC has a passion for teaching, discovery, people, the environment, and the North. UNBC provides outstanding undergraduate and graduate learning opportunities that explore cultures, health, economies, sciences and the environment. As one of B.C.'s research-intensive universities, UNBC brings the excitement of new knowledge to all of its students, and the outcomes of its teaching and research to the world. In addition to fostering and celebrating academic excellence, UNBC is a welcoming place, with a learning environment that is friendly, inclusive, and supportive. UNBC is a university both in and for the north, and this mission has instilled a strong sense of ownership, purpose, and adventure among our students, alumni, faculty, staff, and the communities it serves. UNBC is also Canada's Green University™, leading the way to a more sustainable future for all.

## Master of Engineering in Integrated Wood Design

As part of our contribution to a sustainable future, UNBC introduced The Master of Engineering in Integrated Wood Design program in 2016 to focus on research and education for students and professionals in the field of modern wood structures, including up-to-date structural design with concentration on special fields such as seismic design, hybrid structures, building acoustics, energy efficiency and sustainability. Now in its fourth year and located in the Wood Innovation Design Centre (WIDC) building in Prince George, students are exposed to leading knowledge in the industry, enabling them to actively contribute to the evolution of, and innovation in, the construction industry. By understanding wood at both the micro and macro levels, exploring the science and art of connecting wood and studying the advantages and disadvantages of combining wood with other structural media along with a focus on seismic safety, this program helps students emerge as leaders in environmentally responsible and resource-efficient industrial engineering technologies. Students study iconic structures in the world including those found in British Columbia from both engineering and architectural perspectives and research the applications of wood in the construction of structural systems and envelope design, including insulation, facade, and window and curtain wall systems.

UNBC, through the Master of Engineering Program in Integrated Wood Design, supports BC's wood-related construction industry as a whole. The goal of the program is to foster the development of modern technologies and engineering in the field of structural, envelope, and sustainable design, and to contribute to the development of Northern BC's value-added forest industry.

## Wood Innovation Research Laboratory

UNBC is a leading research university and aims to provide significant research facilities to its students and faculties. The Wood Innovation Research Laboratory (WIRL) building was completed in July of 2018 and is North America's first industrial structure certified under the Passive House certification program. Built using a highly insulated envelope and airtight construction detailing, the finished building was constructed to provide students and faculty of the Integrated Wood Design Program with a facility that can accommodate industry leading testing and research in the field of mass timber engineering and sustainability. The WIRL building was built predominantly using wood and engineered wood-based products including glulam posts and beams and locally sourced ceiling and wall truss systems. To achieve the thermal performance required to meet the Passive House certification standard, a flat truss system typically used for horizontal ceiling assemblies was used vertically to create a thick wall assembly. By using predominantly wood products for the construction of the building, the carbon footprint and associated greenhouse gas emissions were substantially lower than if it had been constructed using concrete and steel and provides

a strong example for the use of wood in buildings traditionally designed for concrete and steel construction. In constructing the WIRL building, advanced testing of wood and engineered wood products, including structural, seismic, acoustic and hygrothermal properties testing may be conducted by staff and students. The WIRL building will continue to maintain a low impact on the environment though energy-use savings due to its construction as a high-performance building certified under the Passive House certification system. It is the intent of this research to demonstrate this performance so that British Columbia can be a leader in the use of wood in our built environment to fight the impacts of climate change and reduce our carbon footprint.

## Passive House Institute

The Passive House Institute is an independent research institute founded in 1996 in Darmstadt, Germany. The purpose of the Passive House Institute is to provide research and development in the construction concepts, building components, planning tools and quality assurance for energy efficient buildings (Passive House Institute, 2015). The Passive House Institute developed certification and training for both professionals and buildings aimed at improving the energy efficiency of the built environment. The Passive House certification for buildings sets strict upper limits on the total non-renewable primary energy demand, thermal energy heating demand and airtightness rates which a building may have. In doing so, the certification encourages an 'envelope-first' approach that results in a reduction of the impact a building may have on the environment through reduced overall energy consumption.'



# Energy Use in Canada

Although secondary energy use increased 23% in the commercial/institutional sector between 1990 and 2013, energy intensity (GJ/m<sup>2</sup>) has decreased by 15% (Natural Resources Canada, 2013). The greatest share of the energy demand by the commercial/institutional sector is space heating, which accounts for 55% of the end-use demand (Figure 1). Although energy intensity has decreased, the built environment still accounts for approximately 25% of the total primary energy use demand in Canada, with 14% of the total end-use demand coming from residential energy use and 12% coming from the commercial sector. The commercial sector is a broad category that includes offices, stores, warehouses, government and institutional buildings, utilities, communications, and other service industries, and also includes energy consumed by street lighting and pipelines (National Energy Board, 2017).

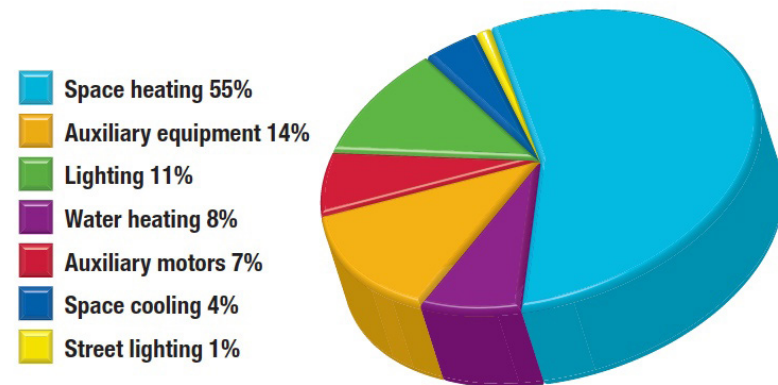


Figure 1. Commercial/institutional energy use by end use, 2013 (Natural Resources Canada, 2013).

In the 2018 CleanBC report, the Government of British Columbia projected a 40% reduction in emissions from buildings within the province through the implementation of energy efficient standards for new construction and clean-energy retrofits (Government of British Columbia, 2018). Additional funding for low-carbon buildings and innovation of low-carbon building solutions has also been implemented.

Currently, 63% of residential and 55% of commercial/institutional energy end use comes from space heating demands (Natural Resources Canada, 2013). By improving the thermal performance of a building's envelope and increasing the airtightness rate, a significant impact can be made on a building's greenhouse gas emissions. By reducing building energy end-use demand, the associated carbon footprint and greenhouse gas emissions of our built environment are reduced. This is important to consider for the lifetime of the building (operational energy use), but also for the construction and future demolition of the building. To reduce the impact of construction and demolition, the materials used in the building's construction must also be taken into consideration. Through advancement in engineering and policy development, several provinces within Canada are leading the market in the use of wood and engineered wood products in residential and commercial building construction. By coupling energy efficient targets with renewable construction materials, the impact of new construction in Canada can be greatly reduced.

# Research and Data Collection


The Passive House Planning Package (PHPP), a static simulation software, was used throughout the design process to predict the energy consumption of the equipment installed in the WIRL and the energy performance of the building itself. PHPP is known for being a very accurate tool to calculate future energy consumption of a building; it is not a dynamic simulation tool, but given its relative simplicity it offers a high level of accuracy. Based on the construction of the building envelope, PHPP provides precise simulation of the thermal energy demand of the building and detailed estimation of the energy load for all energy processes, including lighting, appliances and electronic equipment and mechanical systems operation. The completion of a PHPP model and confirmation of the estimated thermal energy demand and primary energy demand is mandatory for Passive House Certification.

To calculate the natural gas and electric consumption for auxiliary systems for heating (or cooling) purposes, ISO 13790 is used to balance all thermal losses through opaque and transparent envelope components, ventilation losses and solar heat gains as well as internal heat gains to establish the remaining specific heating (or cooling) demand and the heating (or cooling) load of the mechanical equipment. For the calculation of the internal heat gains the type, power and user intervals of all equipment such as lights, plug loads for computers and miscellaneous equipment is calculated. Of particular interest for the WIRL building PHPP model and certification was the energy consumption of the workshop and testing equipment. The use of saws, sanders, shapers and various other tools had to be estimated. By far the largest energy consumers are the Hundegger CNC machine, the hydraulic power unit and actuators for the structural testing and the dust extraction system. The user cycles had to be estimated carefully. Table 1 shows the estimated use and energy consumption of the main components of the specialty equipment.

Equipment	Days of Use [d]	Consumption [kWh]	Electricity Demand [kWh/a]
Wood Shop Equipment	200	77.86	15572
Dust Extraction	200	12.75	2550
Hydraulic Power	100	87.9	8790
Network Equipment	365	3.48	1270

Table 1. Energy Consumption of special Equipment estimated in PHPP.

The PHPP model predicted a Heating Demand of 12 kWh/(m<sup>2</sup>a), a Heating Load of 10 W/m<sup>2</sup> and an overall Primary Energy Demand of 116 kWh/(m<sup>2</sup>a) based on a climate model that uses the average weather data of the last 10 years (Figure 2). Under specific circumstances when energy intensive equipment is used extensively in the summer months, a potential cooling load of 1 W/m<sup>2</sup> was predicted as well.



<b>Building:</b> Wood Innovation Research Laboratory	Street:	1153 4th Avenue
Postcode/City:	V2L 3J2	Prince George
Province/Country:	BC	CA-Canada
Building type:	Research Laboratory	
Climate data set:	CA0018b-Prince George	
Climate zone:	2: Cold	Altitude of location: 576 m
<b>Home owner / Client:</b> University of Northern British Columbia	Street:	3333 University Way
Postcode/City:	V2N 4Z9	Prince George
Province/Country:	BC	CA-Canada
<b>Mechanical engineer:</b> Stantec	Street:	1100 - 111 Dunsmuir Street
Postcode/City:	V6B 6A3	Vancouver
Province/Country:	BC	CA-Canada
<b>Certification:</b> Herz & Lang GmbH	Street:	Ritzsonnenhalb 5a,
Postcode/City:	87480	Weitnau
Province/Country:	Bavaria	Germany

Architecture:	Stantec	Street:	1100 - 111 Dunsmuir Street
Postcode/City:	V6B 6A3	Vancouver	
Province/Country:	BC	CA-Canada	
<b>Energy consultancy:</b> Stantec	Street:	1100 - 111 Dunsmuir Street	
Postcode/City:	V6B 6A3	Vancouver	
Province/Country:	BC	CA-Canada	
Year of construction:	2018	Interior temperature winter [°C]:	15.4
No. of dwelling units:	1	Interior temp. summer [°C]:	25.0
No. of occupants:	29.0	Internal heat gains (IHG) heating case [W/m²]:	3.2
		Specific capacity [Wh/K per m² TFA]:	84
		IHG cooling case [W/m²]:	3.2
		Mechanical cooling:	x

Specific building characteristics with reference to the treated floor area		Criteria	Alternative criteria	Fulfilled? <sup>2</sup>
<b>Space heating</b>	Treated floor area m²	1041.5		
	Heating demand kWh/(m²a)	12	15	yes
	Heating load W/m²	10	-	10
<b>Space cooling</b>	Cooling & dehum. demand kWh/(m²a)	0	15	15
	Cooling load W/m²	1	-	11
	Frequency of overheating (> 25 °C) %	-	-	-
	Frequency of excessively high humidity (> 12 g/kg) %	0	10	yes
<b>Airtightness</b>	Pressurization test result n <sub>50</sub> 1/h	0.1	0.6	yes
<b>Non-renewable Primary Energy (PE)</b>	PE demand kWh/(m²a)	116	120	yes
<b>Primary Energy Renewable (PER)</b>	PER demand kWh/(m²a)	61	-	-
	Generation of renewable energy (in relation to projected building kWh/(m²a) footprint area)	0	-	-

<sup>2</sup> Empty field; Data missing; -: No requirement

I confirm that the values given herein have been determined following the PHPP methodology and based on the characteristic values of the building. The PHPP calculations are attached to this verification.

**Passive House Classic?**  **yes**

Task: 2-Certifier      First name: Florian      Surname: Lang      Signature: \_\_\_\_\_  
 Certificate ID: 18505-18514\_HUL\_PH\_20180706\_FL      Issued on: 06-07-18      City: Weitnau

Figure 2. Verification Page of PHPP.

Furthermore, these calculations are based on the assumption that all rooms besides the large laboratory space itself, the seminar room, the offices and other rooms, are heated to 20°C. The workshop itself has a reduced temperature of 15.5°C to allow for thermally comfortable working conditions in the winter.

## Building Monitoring

The decision to implement an environmental sensor network to monitor the WIRL building was made before the foundation for the building had been laid. Because we could not rely on more standard mounting practices for the sensor system given the predominantly wooden nature of the building, the sensor network was designed to fit the needs of the WIRL building.

The sensor system was intended to be integrated into the envelope of the building and effectively non-removable after installation. The wiring terminal for each sensor bundle protrudes through the given assembly and is connected to a Raspberry Pi controller. The wiring terminals for the sensor bundles which were installed in the exterior walls were tightly sealed once installed to ensure the air barrier of the envelope was not compromised. By installing several sensor bundles in both the north and south wall assemblies, it was ensured that a certain amount of redundancy existed both for data verification and continued data collection should one sensor fail.

All sensors were chosen in order to communicate with the Inter-Integrated Circuit (I 2C) bus on a Raspberry Pi 3 controller. The I 2C bus allows multiple slave devices to communicate with a master device via the same data pin. Each slave device has a seven-bit hard-wired I 2C bus address. The master device then polls all available addresses, and when an address corresponding to a slave device is found it returns its data. This choice gave us two direct benefits:

- Fewer wires at the terminal point of each sensor string, allowing each terminal wall-hole to be smaller, and more tightly sealed.
- Since we knew the range of (immutable) addresses of each sensor being attached to our sensor strings, we could automate the detection of these sensors. Since each sensor string could contain widely varying numbers and types of sensors, this greatly decreased the total software deployment time.

## Sensors Used

The factors used to choose sensors were cost, availability, ease of integration, accuracy, and durability in cold weather conditions. The specifications of the sensors that were installed in the WIRL building are listed below:

- Humidity and Temperature Sensor: Sensiron SHT31-D. It can measure humidity with an accuracy of +/- 2%, temperature with an accuracy of +/- 0.3 C.
- Temperature Sensor: High Accuracy MCP9808. It can measure temperature with an accuracy of +/- 0.25 C and re- mains accurate in temperatures between -40 C and +125 C.

## Sensors Wiring

The temperature sensors (MCP9808) and humidity sensors (SHT31-D) were soldered to a four-pole 16-gauge wire. The sensor strings for each assembly terminated at one Raspberry Pi controller located adjacent to the given sensor string bundle located on the north and south exterior walls of the building and southwest corner where the floor sensors were installed. For some of the sensor string bundles the distance between the sensor and controller was relatively significant.

A thick wire gauge was selected because of the large distances between the sensors and controllers to reduce the resistance in the set-up. The length of the wire between each sensor was significantly longer than the actual distance between the sensors to reduce the influence of thermal conductivity of the cables on the sensors. We produced six prototype sensor strings given these specifications (Figure 3), and then sealed each with hot glue to avoid any moisture damage while inside the wall.



Figure 3: Sensor Wires.

## Sensor Testing

In order to initialize the sensors, the I 2C bus is read to discover which addresses are connected to it as stated. Since the address ranges of the sensors which were implemented is known, and since those addresses are constant, we know exactly how many and which sensors are connected to the Pi. This means that as long as we know the address range of all potential environmental sensors, and we have written drivers for those sensors, it does not matter which sensor string has been wired to the Raspberry Pi's I 2C bus. The software will auto detect the sensor and use the correct drivers. This is due to our leveraging the Linux command: `i2cdetect`. We have access to this command due to Raspbian Stretch distribution we have deployed on the Raspberry Pi's.

The first round of hardware prototypes was tested to ensure fully functioning sensor strings could be installed without issue. Several connections were found faulty and produced electrical shorts. The shorts occurred right at the soldered joint of the wires to the connector pins. The soldering technique was refined, and hot glue was applied to the embedded floor sensors in order to insulate and eliminate this cause of potential malfunction. The hot glue ensured that the connections were properly fastened and protected and helped to avoid short circuits. The hot glue reduced the sensitivity of the temperature sensors slightly and increased the reaction time, but the tradeoff in protection against physical damage caused by gravel and other materials on site when compacting the soil was worth the slight decrease in reaction time. A similar method was implemented for all temperature sensors in the walls to decrease sensor bias. After all sensor strings were produced, they were tested again to ensure functionality (Figure 4).

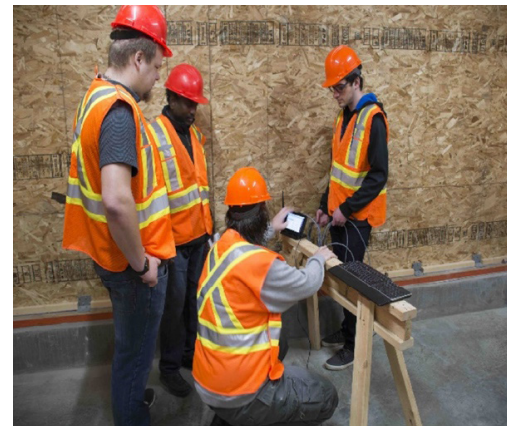


Figure 4: Testing of sensor strings and controllers.

## Experiences and Challenges with Sensors

Early planning soon revealed our two primary architectural issues: scattered terminal deployment, and the physical location of terminal holes. Due to the distance between sensor bundles and controllers a higher gauge of wire had to be utilized to avoid heat and resistance issues since our wiring was now far longer than initially assumed. The physical terminal holes needed to be minimized so that we were not introducing a compromise to the Passive House system in attempting to monitor said system. To that end, we eventually decided on the I 2C bus integrated circuit, thereby reducing the amount of wiring and indirectly reducing the amount of heat introduced to the system.

Deciding between wired or wireless sensors was an early issue raised by the team. Wireless sensors would have avoided complications with moisture wicking between the wires themselves, but would have introduced other, more difficult problems. The connectivity between these sensors couldn't be guaranteed, given their location within the walls and lack of proximity to the Raspberry Pi controllers. We felt that wired communication between terminal and microcontroller was by far the safer option. The challenge was in soldering relatively thick and stiff wires to the very small pins on the sensor microcontrollers.

Though tedious, soldering the sensors to the corresponding vcc, ground, system clock and data wires was relatively painless. Hardware in any form is challenging given the myriad issues that can arise in construction. As our installation team became more experienced with the hardware in question, the entire process became very fluid.

Testing was extensive on the sensor strings prior to installation by necessity. There was only one opportunity to ensure the sensors worked before they were installed in the walls, and once installed we had no ability to retrieve or fix damaged sensors. This is the primary reason we have many redundancies.

## Metering of Energy Consumption

In addition to the sensors which were installed in the southwest corner of the building floor slab and north and south exterior walls, both fuel and electricity consumption meters were installed to measure the energy consumption during the first seven months of operation of the WIRL building. The heating for the building is provided by a radiant in-floor hydronic

loop supplied by a natural gas boiler. A gas consumption meter was installed and data collection began on December 6, 2018. Electrical power to the building is supplied by BC Hydro. An electrical consumption meter was installed and data collection began on July 13, 2018. All data is collected and reported to UNBC's facilities department who then distributes the information to the WIRL research team.

# Discussion

## Energy Consumption of the Wood Innovation Research Lab

To assess the predicted performance of the WIRL building and confirm its eligibility for Passive House certification, a Passive House Planning Package (PHPP) model was completed. Table 2 summarizes the Passive House certification requirements and the final modeled and measured values achieved by the WIRL building. Note that aside from the final air change rate (n50 1/h), all predicted performance values are based on calculations completed by the PHPP software given the inputs entered by the certified modeler and the agreed upon building design.

	WIRL Building	Passive House Criteria	Criteria fulfilled?
Heating demand kWh/(m2a)	12	15	Yes
Cooling & dehumidification demand kWh/(m2a)	0	15	Yes
Pressurization test result (n50 1/h)	0.1	0.6	Yes
Primary Energy demand kWh/(m2a)	116	120	Yes

Table 2. Passive House certification criteria and final modeled and tested results of the WIRL building.

The WIRL building was constructed to serve as a research facility for UNBC faculty and students. The building consists of one large two-bay lab space and several smaller rooms including office and classroom space and washroom facilities distributed between the first floor and a second-floor mezzanine. The building measures 10m in height, and sits on top of a 31m<sup>2</sup> concrete raft slab. The building is equipped with an elevator for access to the second floor mezzanine to provide full accessibility. Additional machinery and equipment included in the predicted annual energy use of the WIRL building include an overhead crane, three Universal Testing Machines (UTM), a Hundegger brand Computer Numerical Controlled (CNC) cutting machine as well as a 34 m<sup>2</sup> wood conditioning room that is equipped with ventilation and humidification in order to create an ideal environment for normalizing wood specimens to a consistent moisture content. Large shipments and deliveries can be received through an overhead bay door.

To maintain a consistent indoor environment, the WIRL building is separated into two climate-controlled zones. The first is the lab and research space, which is maintained at 15C, and the office and classroom space, which are maintained at 20C. Space heating and hot water are provided through a condensing natural gas boiler, while all electricity is provided through hydro power. Ventilation is provided to the building through two heat recovery ventilators (HRVs), which are designed to exhaust stale air and supply fresh air throughout the building.

## Total Space and Hot Water Heating Demand

The space and hot water heating to the WIRL building are supplied by a natural gas condensing boiler. A meter was installed to measure the gas consumption of the building on Dec. 6, 2018. To compare the predicted gas consumption of the building and the actual consumption, we compare the values derived from the PHPP program to weather data for Prince George from Environment Canada on a monthly basis.

Based on the given assumptions for space and hot water use in the building as calculated by the PHPP program, the total specific heating demand is as shown in Figure 5. The actual natural gas consumption as measured by the gas meter installed on the building for the period of December 6 to 31, January 1 to 31 and February 1 to 28 is shown in Figures 6 and 7.

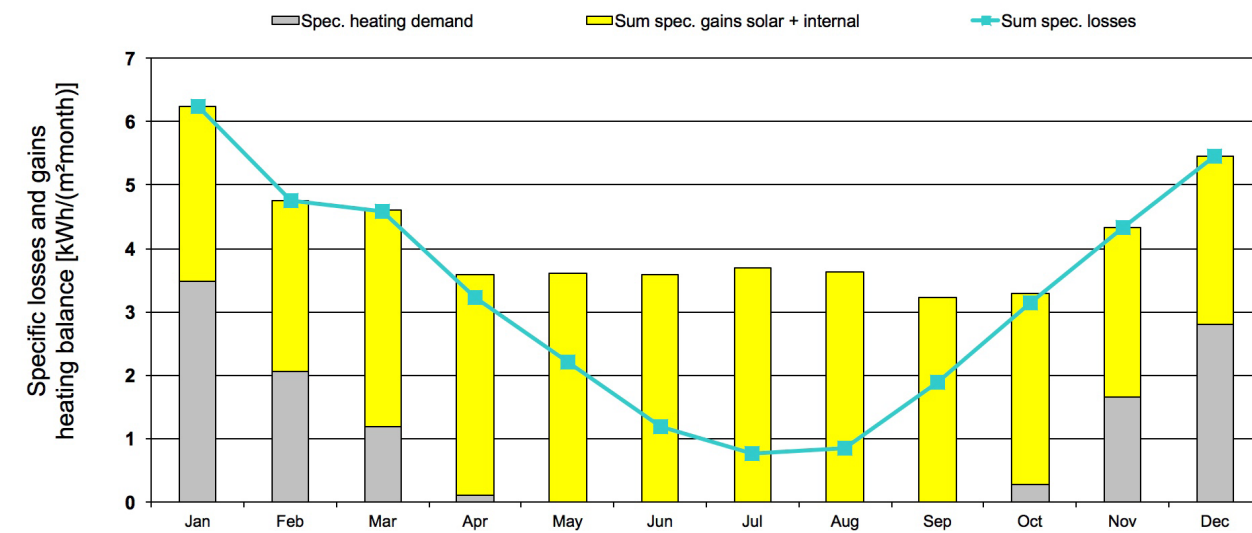


Figure 5. Calculated specific heating demand by month as calculated by the Passive House Planning Package (PHPP) program.

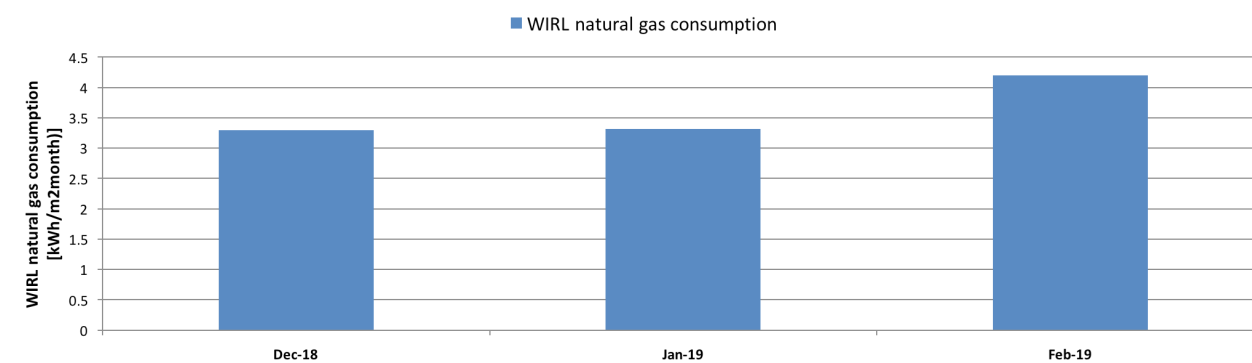


Figure 6. Total monthly gas consumption (kWh/m2month) as collected from the gas meter installed on the WIRL building for the period of Dec. 6 2018 to Feb. 28, 2019.

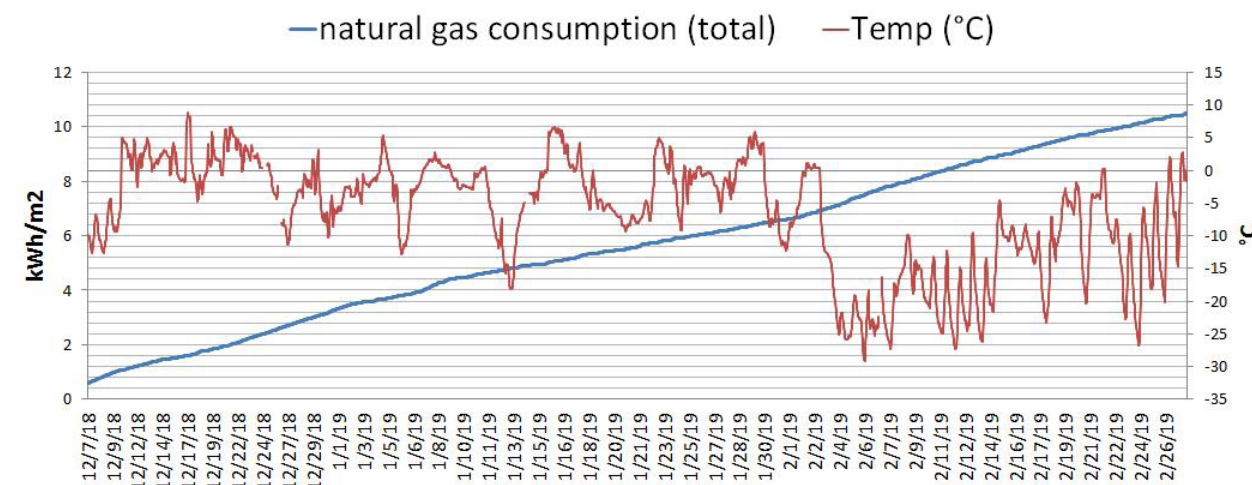


Figure 7. Cumulative natural gas consumption (kWh/m2) vs temperature (°C) for the period of Dec. 7 to Feb. 28 2019.

When evaluating the predicted values from PHPP versus the known natural gas consumption from the meter installed on the building, we can see the following:

- For the month of December, PHPP predicted a total specific heat demand of 2.8kWh/m2 , or 28916.2kWh of energy use (using a total conditioned floor area of 1041.5m2). In contrast, the meter installed on the building shows a total cumulative consumption of 3.3kWh/m2 of natural gas, or 3436.28kWh.
- For the month of January, the PHPP model predicted a total specific heat demand of 3.5kWh/m2, or 3645.25kWh. The gas meter recorded a total consumption of 3.3kWh/m2, or 3452.53kWh.
- For the month of February, the PHPP model predicted a total specific heat demand of 2.1kWh/m2, or 2187.15kWh. The gas meter recorded a total consumption of 4.2kWh/m2, or 4416kWh.

It is important to review the assumptions made by PHPP when calculating the specific heating demand for the building so that we may better understand the possible cause(s) of the discrepancies found between the modeled and reported values.

The first cause of discrepancy that can be found between the PHPP model and actual performance of the WIRL building is in the climatic data used in the PHPP model versus the actual recorded temperatures for the months during which gas consumption has been recorded. These values can be seen in Figure 8.

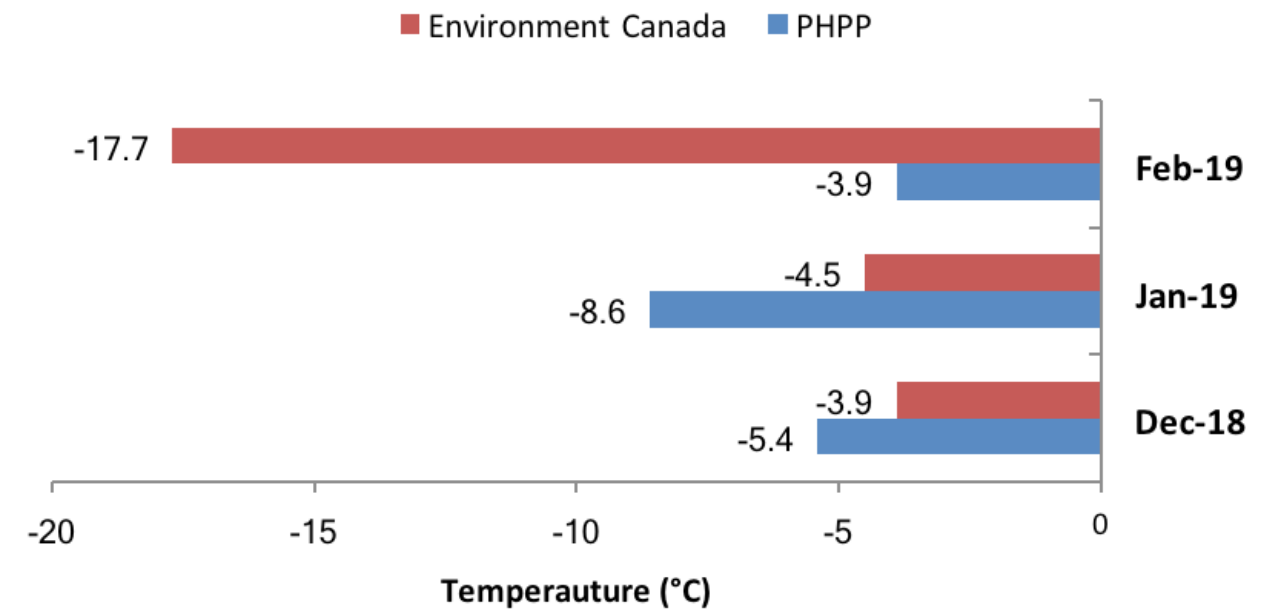


Figure 8. Modeled ambient temperature vs. actual weather data for WIRL building.

From Figure 8 we can see that discrepancies exist between the ambient temperatures used in the PHPP model versus the actual recorded average temperatures for Prince George for the months of December 2018 and January and February of 2019. February 2019 shows a particularly large difference between the two values, which may be accounted for in the fact that it was the coldest February on record in the city's history, with an average temperature of -17.7°C. For the month of January, PHPP used an average ambient temperature of -8.6°C, while the actual measured average temperature was -4.5°C. This is reflected in the heating energy use for the building, which is 0.2kWh/m2 lower than the predicted heating energy demand by PHPP.

For the month of December, we find that the average outdoor temperature was warmer than that used by PHPP as the ambient design temperature; however, the gas consumption for the building is higher than predicted by the PHPP model. In investigating the energy use for the month of December, we see an anomaly in the gas consumption for the first hours in which the gas meter was operational on the building. The total amount of gas used for this period (10:30-14:00 of Dec. 6, 2018), is 1.9527GJ, or 542kWh of gas consumption. We find this to be comparable to the difference in modeled versus

actual gas consumption for the month, which is 520kWh of consumption. In reviewing the consumption data for the remaining reporting period (Figure 9), we find that the consumption is consistent thereafter. Therefore, we feel confident that the discrepancy for energy consumption for the period of December can be accounted for in the startup errors in the gas metering device.

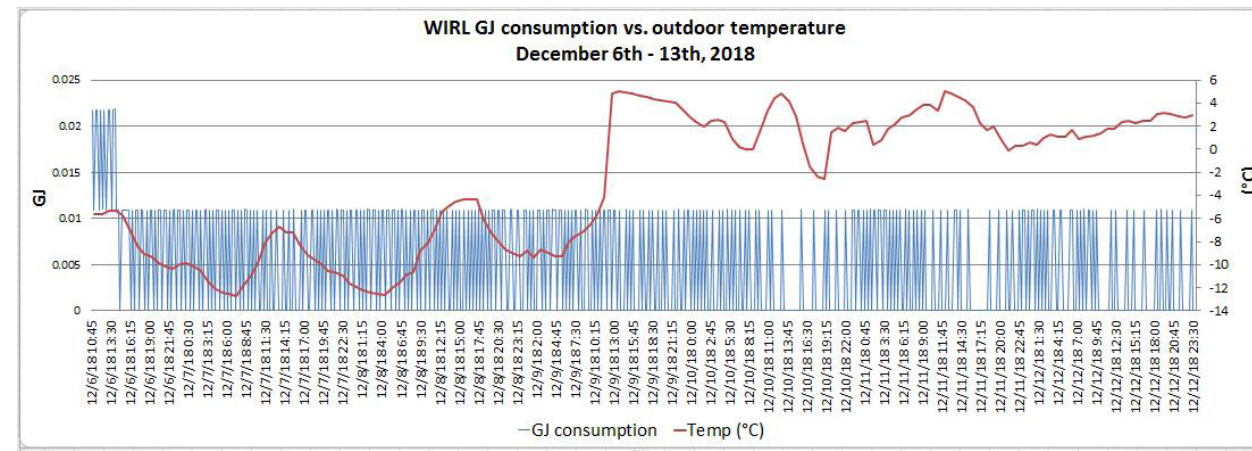


Figure 9. Gas consumption data for WIRL building, recorded on 15min intervals.

## Air Leakage Test Data

Airtightness is an important part of building energy efficiency and the Passive House certification. Air leakage through discontinuities in the primary air barrier can account for 30% or more of a building's heating and cooling costs and contribute to structural durability and indoor air quality problems (U.S. Department of Energy, 2019). In addition, air leakage through the building envelope can lead to long term durability issues when moisture is transported into the wall and ceiling assemblies as well through the process of air leakage. To reduce heat loss from the building and ensure long-term durability, the Passive House certification program requires airtightness rates of 0.6 n50 1/h or less.

Following completion of the building in July of 2018, the WIRL building achieved a final airtightness rate of 0.07 n50 1/h. Points of air leakage through the envelope were identified and included minor penetrations through the wall assembly. The majority of the leakage detected was around the perimeter of the overhead bay door installed on the east wall of the building.

To measure what, if any changes had occurred to the airtight layer since construction was complete, a second, follow up airtightness test was performed on Feb. 6, 2019. The results are shown in Table 3.

Test Direction	Air changes at 50 Pa, n50 1/h
Pressurization	0.1128
Depressurization	0.1717
<b>Final</b>	<b>0.1423</b>

Table 3. Follow up air leakage test results for WIRL building.

As per testing protocol established under the Passive House certification system, both a pressurization and depressurization test must be complete on the building to reflect all possible areas of leakage within the envelope.

## Thermographic Pictures

We conducted an examination of potential weak spots of the envelope in terms of air tightness and thermal bridging with a thermographic camera during the follow up air leakage testing which was conducted on Feb. 6, 2019. The exterior temperature at the time was -29.0C and the interior temperature was 17.5C.

Figure 10 shows the large bay door for semi-trucks. Throughout airtightness testing we established already that this door, even though the highest quality available today, is still a weak point in terms of thermal performance and air tightness. The picture shows the infiltration of cold air in the lower section of the door symmetrically on both sides. It can be assumed that during regular operating condition of the building this area is a significant source of warm air exfiltration.

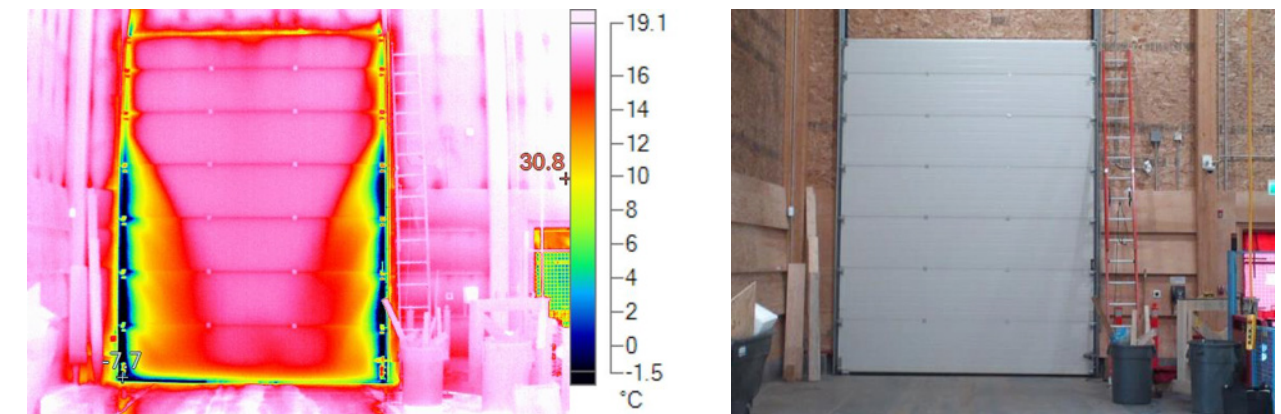


Figure 10. Thermographic image of the WIRL bay door (left) and corresponding visible light image (right) taken during the follow up air leakage test conducted on Feb. 6, 2019.

Figure 11 shows cold air infiltrating mainly on the opening side of the north wall entry door due to a malfunctioning seal between the door and frame.

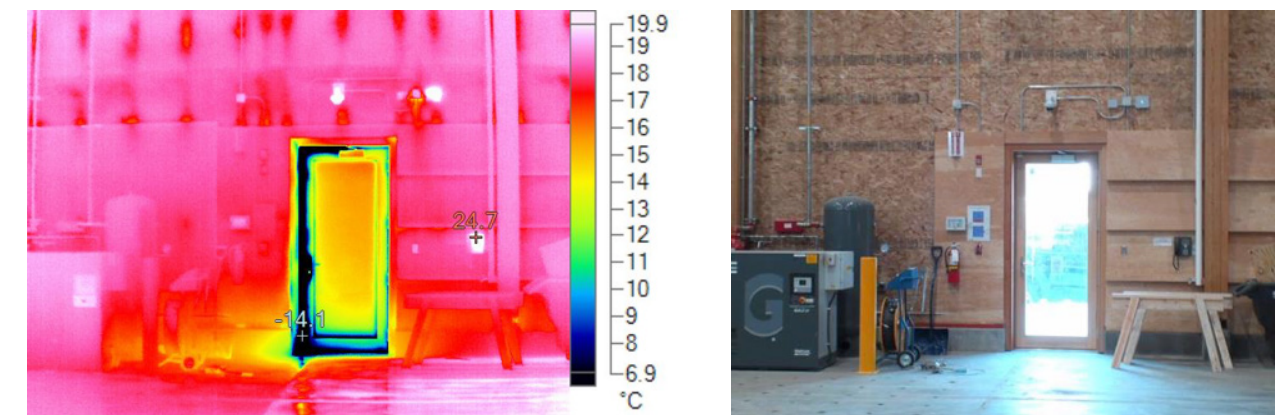


Figure 11. Thermographic image of the north entry door (left) and corresponding visible light image (right) taken during the follow up air leakage test conducted on Feb. 6, 2019.

Figure 12 shows the cold air intake of the Heat Recovery Ventilation System (HRV). It is normal that the cold air intake would show lower temperature since exterior air is sucked into the building through this duct, however in addition we can see some lack of airtightness at the perimeter of the insulated ductwork.

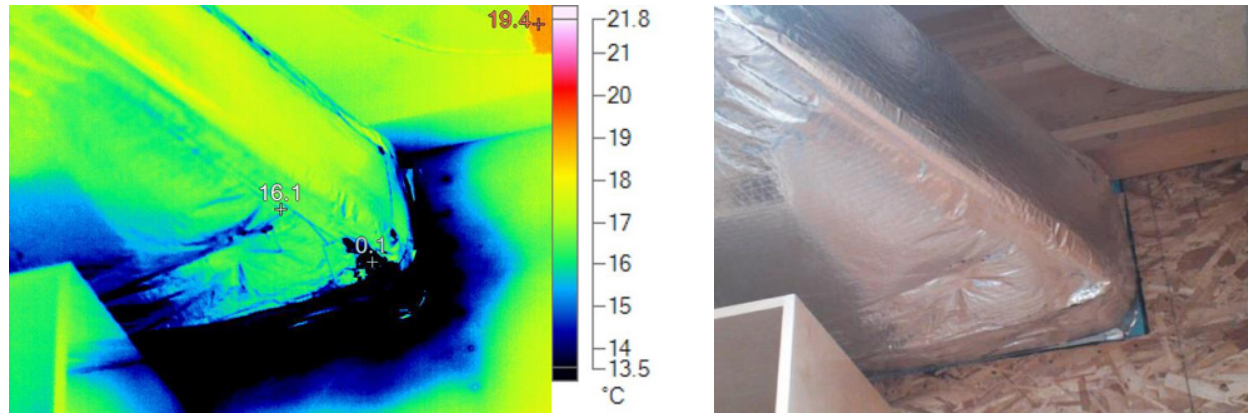


Figure 12. Thermographic image of the HRV cold air intake (left) and corresponding visible light image (right) taken during the follow up air leakage test conducted on Feb 6, 2019.

Figure 13 shows the wall structure and the minor thermal bridges caused by the truss systems of the exterior wall assembly. These point loads are not related to air tightness but a result of the last few remaining thermal bridges in the envelope. The thermal performance of this wall is better than an equivalent stud wall would have been.

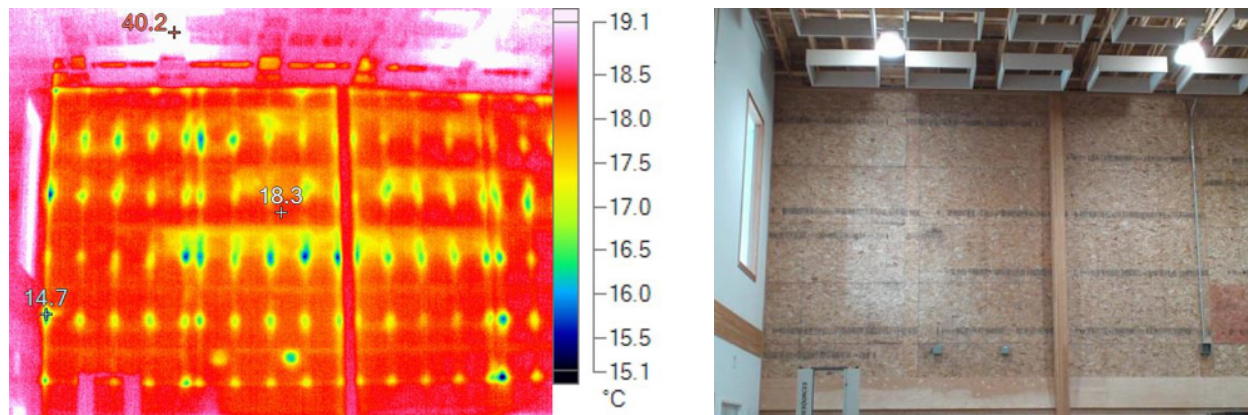
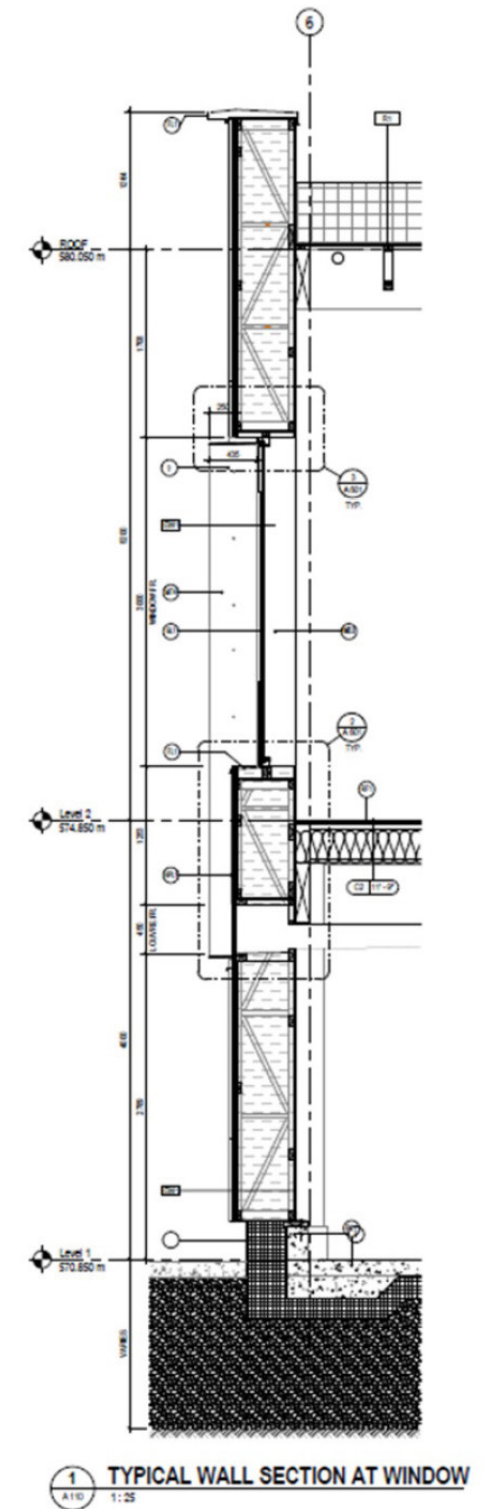


Figure 13. Thermographic image of the west exterior wall (left) and corresponding visible light image (right) taken during the follow up air leakage test conducted on Feb 6, 2019.

### Exterior Wall Assembly Performance

The exterior walls of the Wood Innovation Research Lab were constructed using 508mm thick vertical truss panels filled with mineral fiber insulation. The panels were sheathed on both the interior and exterior side with oriented strand board (OSB), with a vapour diffusion resistant adaptable membrane installed on the exterior face of the interior OSB sheathing for airtightness and vapour diffusion control (Figure 14).

Figure 14. Cross-section diagram of Wood Innovation Research Lab exterior wall.



Temperature and relative humidity sensors were installed in the north and south exterior wall cavities and the southwest corner of the floor assembly to measure the thermal and moisture performance of the exterior wall and floor assemblies. The purpose of the sensor installation was to allow for long-term building performance and energy demand monitoring to provide insights into industrial building construction.



## North Wall

Four separate arrangements of sensors in the north wall were configured with two temperatures and one humidity sensor (N01, N02, N05 and N06) (Figure 15a), and two arrangements were configured with two humidity and one temperature sensors (N03 and N04) (Figure 15b). For configurations N01, N02, N05 and N06, the temperature sensors are located on the exterior face of the interior OSB sheathing layer and the interior face of the exterior OSB sheathing layer, with the humidity sensor located in the center of the insulated assembly. The two additional sensor configurations, N03 and N04, were configured with two humidity sensors and one temperature sensor. Here, the two humidity sensors are located on the exterior face of the interior OSB sheathing layer and the interior face of the exterior OSB sheathing layer, with the temperature sensor located in the center of the insulated assembly.

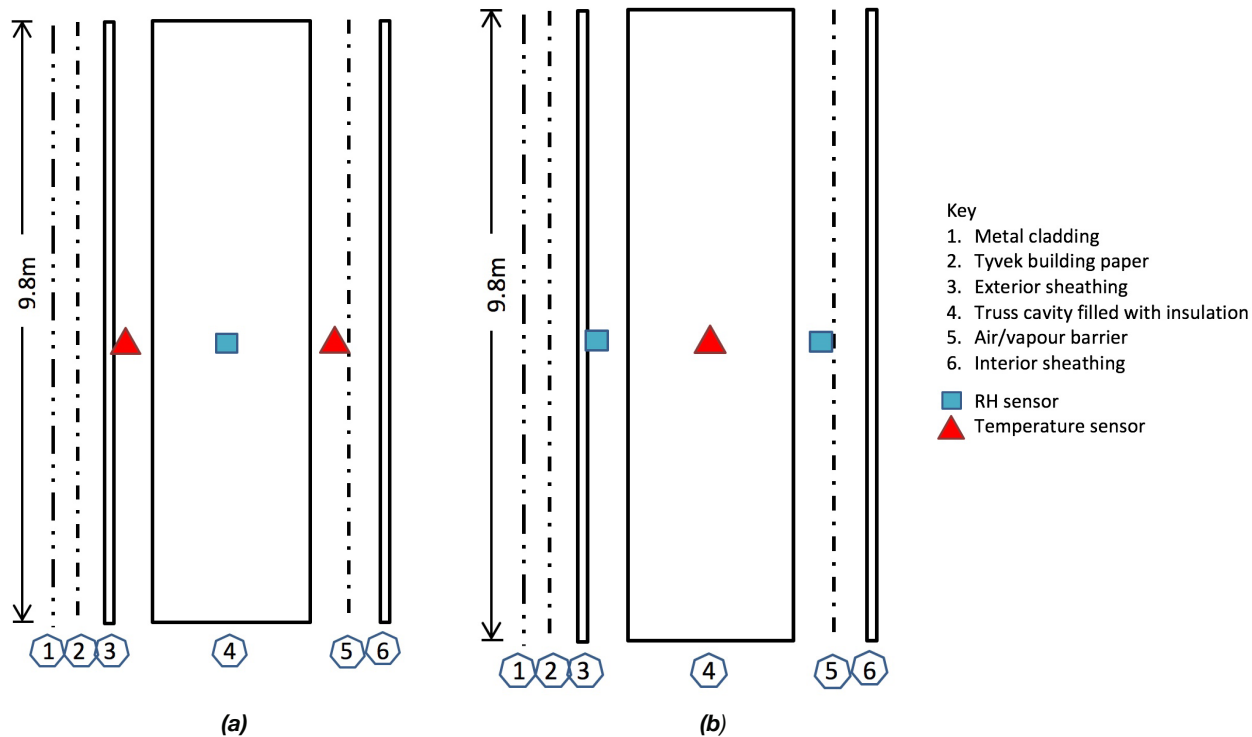


Figure 15. Sensor placement in exterior north and south wall assembly of WIRL building. Sensor groups N01, N02, N05 and N06 and S01, S02, S05 and S06 are configured as shown in (a). Sensor groups N03 and N04 S03 and S04 are configured as shown in (b).

A review of the data collected from the six sensor groups located in the north wall of the WIRL building show that at no point during the reported data collection period of July 18, 2018 to Jan. 12, 2019 was 100 percent saturation (relative humidity) achieved in the wall assembly. The maximum relative humidity value was recorded by sensor N06 on Jan. 8, 2019 at 22:00, with a value of 76.59% (Table 5). This value correlates with one of the greatest differences in temperatures found between the two temperature sensors in the same sensor configuration, indicating a low exterior temperature. This is confirmed by the hourly weather data reported for the city, which shows Jan. 8 was the coldest recorded day between the period of Dec. 5 and Jan. 15 (Figure 16). In a review of the top 10 records of high relative humidity and greatest temperature differences between sensor configurations N01, N02, N05 and N06 (Table 4 and 5) in the north wall, we find that on average 22.5 percent of the highest relative humidity readings correspond with the greatest temperature difference between the associated temperature sensors. In addition, all of the top 10 highest relative humidity recordings from the four wall sensor bundles which are located in the center of the wall assembly occur within the same 8 days for the reporting period. Comparing these to the hourly weather trends shown in Figure 16, we find that an additional four days with the recorded highest humidity readings correspond with cold exterior weather events, including Dec. 9 and 31 and Jan. 7 and 9. Although the two remaining days with recorded high relative humidity, Jan. 10 and 11, do not correspond with cold exterior weather events, the reported data is believed to be a result of the cold weather event that occurred in the days prior and a delay in the movement of moisture across the building assembly.

The two sensor groups in the north wall that are configured with two humidity sensors and one temperature sensor (N03 and N04) show values that support the findings from sensor groups N01, N02, N05 and N06. The greatest difference in humidity recorded between the interior and exterior humidity sensors during the heating season of the reported months occurred on Jan. 8, 2019 (Table 6a and 7a). During the cooling season months, a higher relative humidity on the exterior side of the envelope compared to the interior resulted in an inward movement of moisture through the assembly. This can be seen in Table 6b and 7b, with dates of highest recorded difference in relative humidity occurring during the highest exterior temperature records which occurred between July 27 and 29 and Aug. 5 and 6, 2018 (Figure 17) or immediately thereafter due to a delay in moisture movement across the assembly.

N01		
Top 10	Highest RH	Date
1	67.543	12/9/2018 17:00
2	66.65	12/9/2018 16:00
3	66.639	12/9/2018 18:00
4	66.156	12/31/2018 16:00
5	65.894	1/8/2019 17:00
6	65.857	1/10/2019 16:00
7	65.773	1/10/2019 15:00
8	65.671	1/8/2019 16:00
9	65.554	12/29/2018 16:00
10	65.49	12/31/2018 15:00

N02		
Top 10	Highest RH	Date
1	67.951	1/8/2019 16:00
2	67.895	12/9/2018 16:00
3	67.777	1/8/2019 15:00
4	67.343	1/8/2019 17:00
5	67.328	12/31/2018 15:00
6	67.2	12/9/2018 17:00
7	67.154	1/7/2019 15:00
8	66.823	12/31/2018 16:00
9	66.755	1/10/2019 15:00
10	66.625	1/8/2019 14:00

Top 10	Highest ΔT	Date
1	-15.119	1/8/2019 12:00
2	-15.104	1/8/2019 13:00
3	-15.104	1/8/2019 11:00
4	-15.073	1/8/2019 10:00
5	-15.021	1/8/2019 14:00
6	-14.937	1/8/2019 15:00
7	-14.915	1/8/2019 9:00
8	-14.844	1/8/2019 16:00
9	-14.713	1/8/2019 17:00
10	-14.708	1/8/2019 8:00

Top 10	Highest ΔT	Date
1	-12.646	1/8/2019 16:00
2	-12.642	1/8/2019 17:00
3	-12.599	1/8/2019 15:00
4	-12.557	1/8/2019 18:00
5	-12.453	1/8/2019 14:00
6	-12.302	1/8/2019 19:00
7	-12.262	1/8/2019 13:00
8	-12.167	1/8/2019 20:00
9	-12.12	1/8/2019 21:00
10	-12.083	1/8/2019 12:00

Table 4. Top 10 highest relative humidity (RH) and temperature differences (ΔT) between the sensors located in configurations N01 and N02. Highlighted values indicate corresponding occurrence between highest RH and ΔT for each sensor group.

N05		
Top 10	Highest RH	Date
1	72.741	12/9/2018 18:00
2	72.692	12/9/2018 17:00
3	71.932	12/9/2018 19:00
4	71.196	12/9/2018 20:00
5	71.11	12/9/2018 16:00
6	70.538	12/9/2018 21:00
7	70.427	1/10/2019 16:00
8	70.42	1/11/2019 15:00
9	70.259	1/10/2019 17:00
10	70.185	1/9/2019 16:00

N06		
Top 10	Highest RH	Date
1	76.59	1/8/2019 22:00
2	76.59	1/8/2019 23:00
3	76.549	1/8/2019 18:00
4	76.501	12/9/2018 17:00
5	76.483	1/9/2019 0:00
6	76.475	1/8/2019 17:00
7	76.383	1/9/2019 1:00
8	76.37	1/8/2019 19:00
9	76.358	1/8/2019 21:00
10	76.352	12/31/2018 16:00

Top 10	Highest ΔT	Date
1	-15.375	1/8/2019 16:00
2	-15.318	1/8/2019 15:00
3	-15.313	1/8/2019 17:00
4	-15.125	1/8/2019 14:00
5	-15.109	1/8/2019 18:00
6	-14.909	1/8/2019 13:00
7	-14.693	1/8/2019 19:00
8	-14.682	1/8/2019 12:00
9	-14.433	1/8/2019 11:00
10	-14.398	1/8/2019 20:00

Top 10	Highest ΔT	Date
1	-18.703	1/8/2019 15:00
2	-18.654	1/8/2019 16:00
3	-18.578	1/8/2019 17:00
4	-18.52	1/8/2019 14:00
5	-18.244	1/8/2019 18:00
6	-18.214	1/8/2019 13:00
7	-17.896	1/8/2019 12:00
8	-17.567	1/8/2019 11:00
9	-17.545	1/8/2019 19:00
10	-17.239	1/8/2019 10:00

Table 5. Top 10 highest relative humidity (RH) and temperature differences (ΔT) between the sensors located in configurations N05 and N06. Highlighted values indicate corresponding occurrence between highest RH and ΔT for each sensor group.

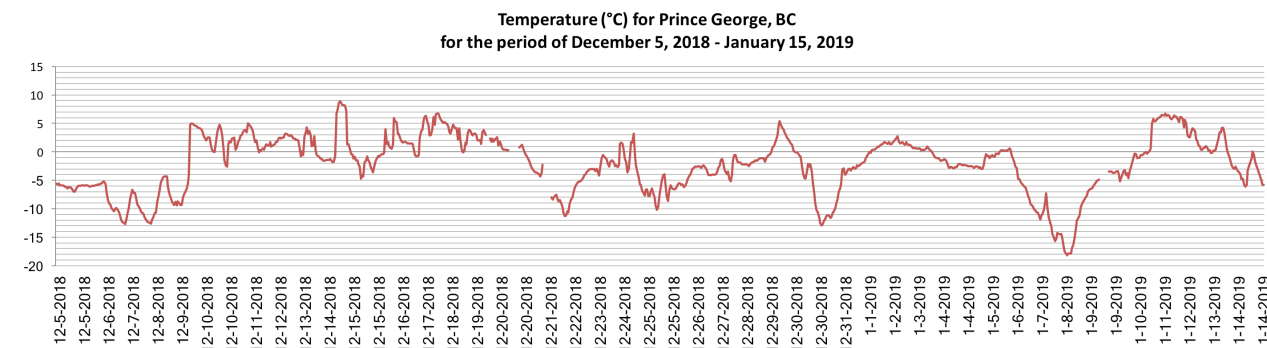


Figure 16. Hourly temperature (°C) for Prince George from Dec. 5, 2018 to Jan. 15, 2019 (Government of Canada, 2019).

N03		
Top 10	Highest RH	Date
1	64.757	2019-01-08 16:00
2	64.735	2019-01-08 15:00
3	64.386	2019-01-08 14:00
4	64.31	2019-01-08 17:00
5	64.286	2018-12-31 16:00
6	64.261	2018-12-31 15:00
7	64.211	2019-01-08 13:00
8	64.112	2019-01-08 11:00
9	64.108	2019-01-08 12:00
10	64.094	2018-12-09 17:00

N03		
Top 10	Highest RH	Date
1	58.033	2018-08-06 18:00
2	58.008	2018-08-06 19:00
3	57.507	2018-08-06 17:00
4	56.927	2018-08-06 20:00
5	56.126	2018-07-30 19:00
6	56.054	2018-07-30 20:00
7	55.955	2018-08-06 16:00
8	55.831	2018-07-30 21:00
9	55.745	2018-07-30 18:00
10	55.657	2018-08-06 21:00

Top 10	Highest ΔT	Date
1	39.366	2019-01-08 14:00
2	39.302	2019-01-08 13:00
3	39.298	2019-01-08 15:00
4	39.064	2019-01-08 12:00
5	38.848	2019-01-08 11:00
6	38.654	2019-01-08 16:00
7	38.55	2019-01-08 10:00
8	37.999	2019-01-08 9:00
9	37.464	2019-01-08 17:00
10	37.445	2019-01-08 8:00

Top 10	Highest ΔT	Date
1	-11.528	2018-08-06 19:00
2	-10.976	2018-08-06 18:00
3	-10.938	2018-08-06 20:00
4	-10.08	2018-08-06 17:00
5	-9.679	2018-08-06 21:00
6	-9.515	2018-07-30 20:00
7	-9.439	2018-07-30 21:00
8	-9.429	2018-07-30 19:00
9	-9.287	2018-08-01 19:00
10	-9.285	2018-07-30 22:00

(a)

(b)

Table 6. The 10 highest recordings of relative humidity and difference in relative humidity ( $\Delta RH$ ) between the sensors located in configuration N03. Values shown in (a) are those for the sensor located towards the exterior side of the assembly, and the greatest differences between the interior-side sensor and exterior-side sensor, indicating a movement of moisture outward through the assembly. Values shown in (b) are those for the sensor located towards the interior side of the assembly and the greatest differences between the exterior-side sensor and interior-side sensor, indicating a movement of moisture inward through the assembly.

N03			N03		
Top 10	Highest RH	Date	Top 10	Highest RH	Date
1	72.537	2019-01-08 16:00	1	59.991	2018-08-06 18:00
2	72.396	2019-01-08 15:00	2	59.924	2018-08-06 19:00
3	72.316	2019-01-08 17:00	3	59.142	2018-08-06 17:00
4	71.956	2019-01-08 18:00	4	58.554	2018-08-06 20:00
5	71.949	2019-01-08 14:00	5	58.093	2018-07-27 21:00
6	71.565	2019-01-08 19:00	6	58.079	2018-07-27 20:00
7	71.52	2019-01-08 13:00	7	57.388	2018-07-30 20:00
8	71.474	2019-01-08 21:00	8	57.375	2018-07-27 19:00
9	71.473	2019-01-08 22:00	9	57.355	2018-07-30 19:00
10	71.32	2019-01-08 20:00	10	57.251	2018-08-06 16:00

Top 10	Highest $\Delta T$	Date	Top 10	Highest $\Delta T$	Date
1	46.096	2019-01-08 14:00	1	-17.688	2018-08-06 19:00
2	46.08	2019-01-08 13:00	2	-17.575	2018-08-06 18:00
3	45.854	2019-01-08 12:00	3	-16.458	2018-08-06 17:00
4	45.554	2019-01-08 15:00	4	-15.947	2018-08-06 20:00
5	45.552	2019-01-08 11:00	5	-14.706	2018-07-27 21:00
6	45.263	2019-01-08 10:00	6	-14.497	2018-07-27 20:00
7	44.713	2019-01-08 9:00	7	-14.127	2018-08-08 19:00
8	44.39	2019-01-08 16:00	8	-14.092	2018-07-30 20:00
9	44.111	2019-01-08 8:00	9	-14.01	2018-07-30 19:00
10	43.641	2019-01-08 7:00	10	-13.959	2018-08-08 20:00

(a) (b)

Table 7. The 10 highest recordings of relative humidity and difference in relative humidity ( $\Delta RH$ ) between the sensors located in configuration N04. Values shown in (a) are those for the sensor located towards the exterior side of the assembly, and the greatest differences between the interior-side sensor and exterior-side sensor, indicating a movement of moisture outward through the assembly. Values shown in (b) are those for the sensor located towards the interior side of the assembly and the greatest differences between the exterior-side sensor and interior-side sensor, indicating a movement of moisture inward through the assembly.

Hourly temperature ( $^{\circ}\text{C}$ ) for Prince George, BC for the period of July 15 - September 15, 2019

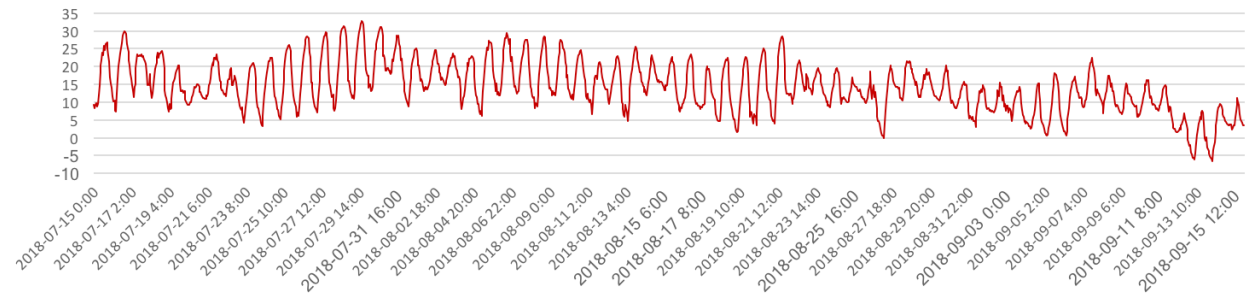


Figure 17. Hourly temperature ( $^{\circ}\text{C}$ ) for Prince George from July 15 to Sept. 15, 2019 (Government of Canada, 2019).

### South Wall

Four separate arrangements of sensors in the south wall were configured with two temperature and one humidity sensor (S01, S02, S05 and S06) (Figure 15a), and two arrangements were configured with two humidity and one temperature sensors (S03 and S04) (Figure 15b). For configurations S01, S02, S05 and S06, the temperature sensors are located on the exterior face of the interior OSB sheathing layer and the interior face of the exterior OSB sheathing layer, with the humidity sensor located in the center of the insulated assembly. The two additional sensor configurations, S03 and S04, were configured with two humidity sensors and one temperature sensor. Here, the two humidity sensors are located on the exterior face of the interior OSB sheathing layer and the interior face of the exterior OSB sheathing layer, with the temperature sensor located in the center of the insulated assembly.

Upon review of the data collected by the south wall sensor configurations, it was discovered that sensor S01 was not transmitting data and no values have been collected. Additionally, sensor S05 transmitted data for two days, July 19 and July 20, 2018, before encountering a malfunction or error that resulted in no further data being reported. Therefore no data is presented for these two sensor configurations.

The four remaining sensor groups located in the south wall of the WIRL building show that at no point during the period of July 18, 2018 to Jan. 12, 2019 was 100 percent saturation (relative humidity) achieved in the wall assembly (Table 8-10). The maximum relative humidity value recorded was by sensor S03 on Jan. 7, 2019 at 17:00 at 94.24% (Table 9a). Similar to the findings of the data reported in the north wall sensors, this value correlates with one of the coldest exterior weather periods reported for the reporting period (Figure 16).

Looking at the data collected by sensors S06, we find that four of the 10 greatest occurrences of high relative humidity recorded correspond with the greatest temperature difference between the interior and exterior of the WIRL building on January 8, 2019 (Table 8). An additional five readings recorded by the sensor also occurred on the same day. Similar to the findings discussed above for the north wall sensor configurations, we find that the remaining days which fall in the top 10 readings for the highest humidity values recorded occur on days following cold weather events. This is believed to be due to the delay in time as the moisture found inside the building migrates across the wall assembly and is recorded by the relevant sensor.

The data from sensor S02 shows no correlations between the dates when the highest recorded relative humidity within the wall assembly occurred and the records for the greatest temperature difference during the reporting period (Table 8). Similar to the conclusions drawn for the other south and north wall sensors, we find that the dates on which the highest relative humidity recordings were made correlate to or follow cold weather events.

The two sensor groups in the south wall which are configured with two humidity sensors and one temperature sensor (S03 and S04) show values that support the findings from sensor groups S01, S02, S05 and S06. The greatest difference in humidity recorded between the interior and exterior humidity sensors during the heating season occurred immediately

preceding the coldest day during the reporting period on Jan. 7, 2019 (Table 9a and 10a). During the cooling season months, a higher relative humidity on the exterior side of the envelope compared to the interior resulted in an inward movement of moisture through the assembly. This can be seen in Table 9b and 10b, with dates of highest recorded difference in relative humidity occurring during the highest exterior temperature records which occurred between July 27 and 29 and Aug. 5 and 6, 2018 (Figure 17) or immediately thereafter due to a delay in moisture movement across the assembly.

S02		
Top 10	Highest RH	Date
1	77.588	2019-01-07 16:00
2	77.563	2018-12-07 14:00
3	75.659	2018-12-07 15:00
4	72.737	2018-12-04 14:00
5	72.274	2018-12-10 14:00
6	71.336	2018-12-27 15:00
7	71.314	2018-12-07 16:00
8	70.637	2018-12-22 14:00
9	70.116	2018-12-24 14:00
10	70.083	2018-12-23 14:00

S06		
Top 10	Highest RH	Date
1	66.982	2018-12-07 14:00
2	64.601	2019-01-08 14:00
3	63.896	2019-01-08 3:00
4	63.602	2019-01-08 10:00
5	63.46	2019-01-08 13:00
6	63.428	2019-01-08 11:00
7	63.388	2019-01-08 2:00
8	63.343	2019-01-08 12:00
9	63.334	2019-01-08 4:00
10	63.088	2019-01-08 9:00

Top 10	Highest ΔT	Date
1	-16.438	2019-01-08 15:00
2	-16.432	2019-01-08 14:00
3	-16.203	2019-01-08 16:00
4	-16.057	2019-01-08 13:00
5	-15.881	2019-01-08 17:00
6	-15.526	2019-01-08 18:00
7	-15.5	2019-01-08 12:00
8	-15.233	2019-01-08 19:00
9	-15.109	2019-01-09 0:00
10	-15.078	2019-01-08 23:00

Top 10	Highest ΔT	Date
1	-14.771	2019-01-08 15:00
2	-14.688	2019-01-08 16:00
3	-14.604	2019-01-08 14:00
4	-14.469	2019-01-08 17:00
5	-14.36	2019-01-08 13:00
6	-14.261	2019-01-08 18:00
7	-14.046	2019-01-08 12:00
8	-13.953	2019-01-08 19:00
9	-13.797	2019-01-08 11:00
10	-13.687	2019-01-08 20:00

Table 8. The top 10 highest relative humidity (RH) and temperature differences (ΔT) between the sensors located in configurations S02 and S06. Highlighted values indicate corresponding occurrence between highest RH and ΔT for each sensor group.

S03		
Top 10	Highest RH	Date
1	94.24	2019-01-07 17:00
2	91.09	2018-12-27 16:00
3	89.977	2018-12-24 16:00
4	89.009	2018-12-07 16:00
5	88.898	2018-12-10 16:00
6	88.67	2018-11-19 15:00
7	88.651	2018-12-30 15:00
8	88.153	2018-11-22 16:00
9	87.735	2018-12-30 16:00
10	87.426	2018-12-23 15:00

S03		
Top 10	Highest RH	Date
1	85.886	2018-07-28 21:00
2	85.573	2018-07-29 21:00
3	85.555	2018-07-27 21:00
4	85.477	2018-07-28 22:00
5	85.402	2018-07-27 22:00
6	84.738	2018-07-29 20:00
7	84.419	2018-07-28 20:00
8	84.125	2018-07-27 20:00
9	83.938	2018-07-27 23:00
10	83.883	2018-07-30 21:00

Top 10	Highest ΔT	Date
1	63.347	2019-01-07 17:00
2	58.087	2018-12-07 16:00
3	57.205	2018-12-27 16:00
4	54.589	2018-12-23 15:00
5	54.522	2019-01-07 16:00
6	54.457	2018-12-30 15:00
7	52.899	2018-12-07 15:00
8	51.897	2018-12-24 16:00
9	51.606	2018-11-19 15:00
10	51.526	2018-12-10 15:00

Top 10	Highest ΔT	Date
1	-47.7	2018-07-28 22:00
2	-47.502	2018-07-30 22:00
3	-47.306	2018-07-28 23:00
4	-47.053	2018-07-30 23:00
5	-46.375	2018-07-30 21:00
6	-46.296	2018-07-27 23:00
7	-46.27	2018-07-29 21:00
8	-46.112	2018-07-27 22:00
9	-45.689	2018-07-29 0:00
10	-45.666	2018-07-28 21:00

(a)

(b)

Table 9. The 10 highest recordings of relative humidity and difference in relative humidity (ΔRH) between the sensors located in configuration S03. Values shown in (a) are those for the sensor located towards the exterior side of the assembly, and the greatest differences between the interior-side sensor and exterior-side sensor, indicating a movement of moisture outward through the assembly. Values shown in (b) are those for the sensor located towards the interior side of the assembly and the greatest differences between the exterior-side sensor and interior-side sensor, indicating a movement of moisture inward through the assembly.

S04		
Top 10	Highest RH	Date
1	72.904	2019-01-07 16:00
2	70.857	2018-12-07 14:00
3	70.076	2018-12-07 15:00
4	68.371	2018-12-22 14:00
5	67.383	2018-12-27 15:00
6	67.256	2018-12-30 14:00
7	67.154	2018-12-04 14:00
8	66.891	2018-12-07 16:00
9	66.693	2018-12-10 14:00
10	66.653	2018-12-24 14:00

S04		
Top 10	Highest RH	Date
1	88.341	2018-07-27 21:00
2	88.138	2018-07-27 20:00
3	86.114	2018-07-30 20:00
4	85.919	2018-07-27 22:00
5	85.688	2018-07-30 21:00
6	85.55	2018-08-05 20:00
7	85.309	2018-07-27 19:00
8	84.579	2018-08-05 21:00
9	83.642	2018-07-30 19:00
10	83.08	2018-07-30 22:00

Top 10	Highest ΔT	Date
1	43.492	2019-01-07 16:00
2	43.032	2018-12-07 14:00
3	40.628	2018-12-07 15:00
4	39.577	2019-01-08 14:00
5	39.017	2019-01-08 15:00
6	38.974	2018-12-22 14:00
7	38.151	2019-01-08 16:00
8	37.819	2018-12-08 14:00
9	37.791	2018-12-08 15:00
10	37.153	2019-01-08 13:00

Top 10	Highest ΔT	Date
1	-55.134	2018-07-27 21:00
2	-55.014	2018-07-30 21:00
3	-54.915	2018-07-30 20:00
4	-54.186	2018-07-27 20:00
5	-53.311	2018-08-05 20:00
6	-53.169	2018-08-05 21:00
7	-52.663	2018-07-27 22:00
8	-52.271	2018-07-30 22:00
9	-50.508	2018-08-20 20:00
10	-50.278	2018-07-30 19:00

Table 10. The 10 highest recordings of relative humidity and difference in relative humidity ( $\Delta RH$ ) between the sensors located in configuration S04. Values shown in (a) are those for the sensor located towards the exterior side of the assembly, and the greatest differences between the interior-side sensor and exterior-side sensor, indicating a movement of moisture outward through the assembly. Values shown in (b) are those for the sensor located towards the interior side of the assembly and the greatest differences between the exterior-side sensor and interior-side sensor, indicating a movement of moisture inward through the assembly.

### Southwest Floor

Six strings of temperature and humidity sensors were installed in a layered grid along the southwest corner of the foundation. The sensor configurations were laid out in parallel lines located in the floor of the conditioning room in the southwest corner of the building, with each line comprising of two sets of six sensors stacked on top of each other above and below the foundation insulation installed under the concrete floor (Figure 18 and 19). This setup allows for an accurate monitoring of heat transfer through the foundation into the soil. This particular location was chosen to use the advantage of the conditioning room because only in this room will the temperature and humidity be stably maintained through the entire year.

After reviewing the data collected by the sensors installed in the floor it was determined that four of the sensor configurations (W01, W02, W03 and W06) had experienced problems and were no longer functioning. It was also found that the humidity sensors installed in the W04 and W05 sensor configurations were not properly functioning either.

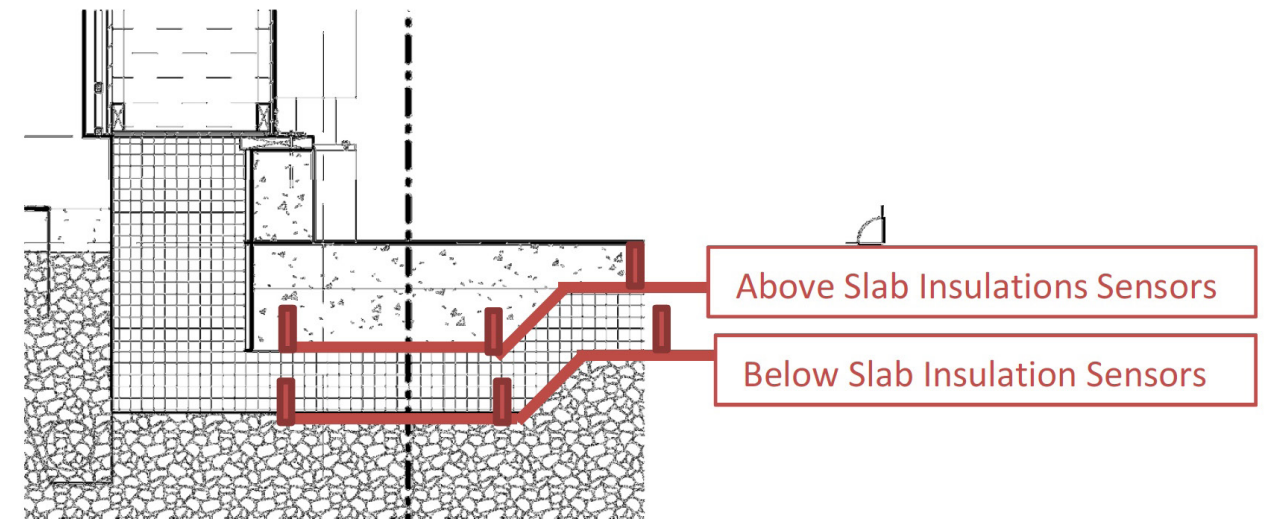


Figure 18. WIRL floor sensor configuration. Sensors are located in a stacked format in two separate parallel lines located in the southwest corner of the building floor.

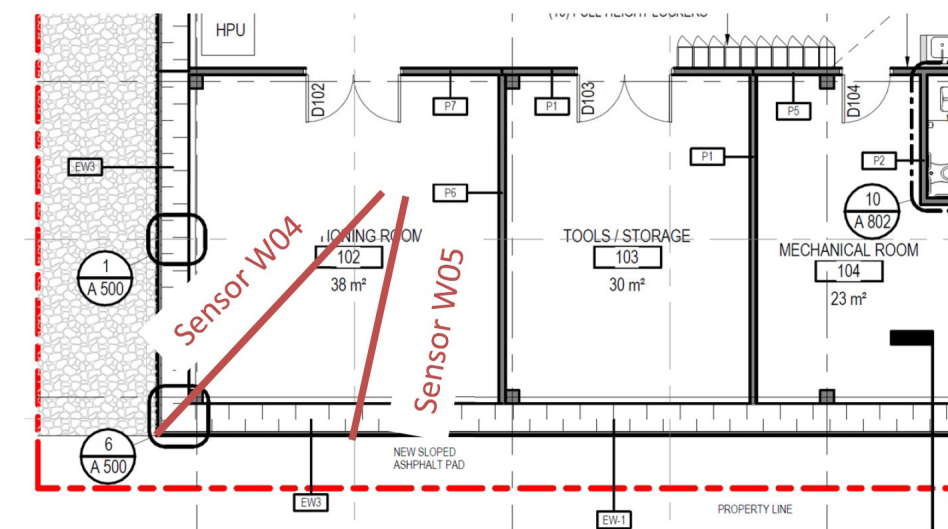


Figure 19. WIRL floor sensor configuration. Sensors are located in a stacked format in two separate parallel lines (labeled as Sensor W04 and W05) located in the southwest corner of the building floor.

The results of the readings from the six sensors in each of the floor sensor configurations are shown in Figure 20 and 21.

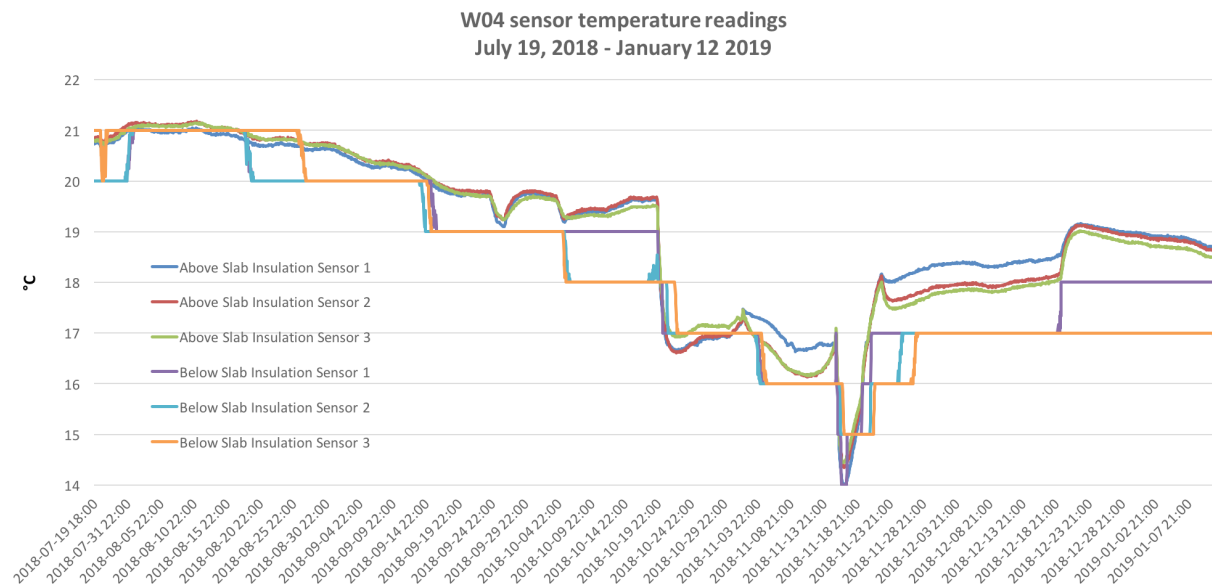


Figure 20. W04 floor sensor temperature readings for the period of July 19, 2018 to Jan. 12, 2019.

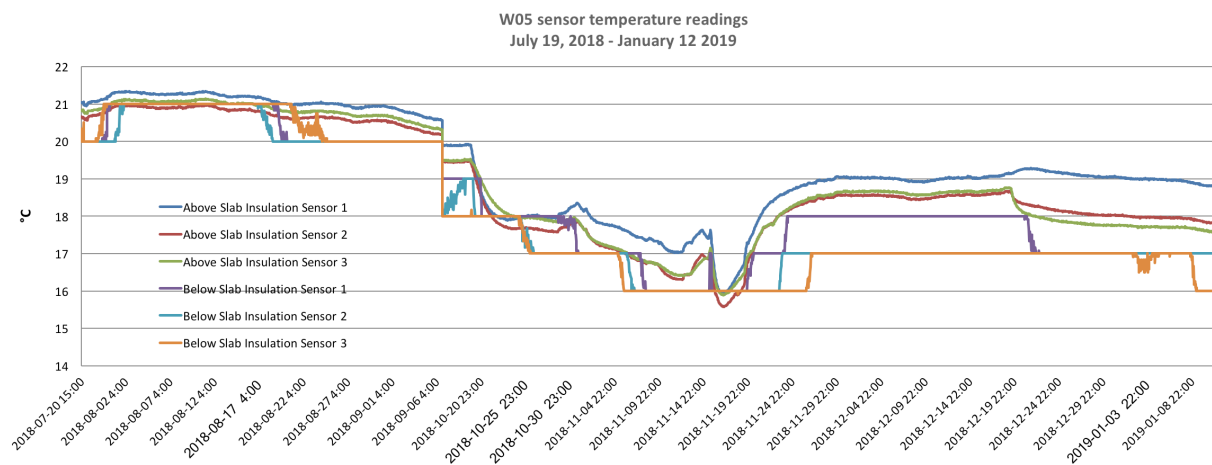


Figure 21. W04 floor sensor temperature readings for the period of July 19, 2018 to Jan. 12, 2019.

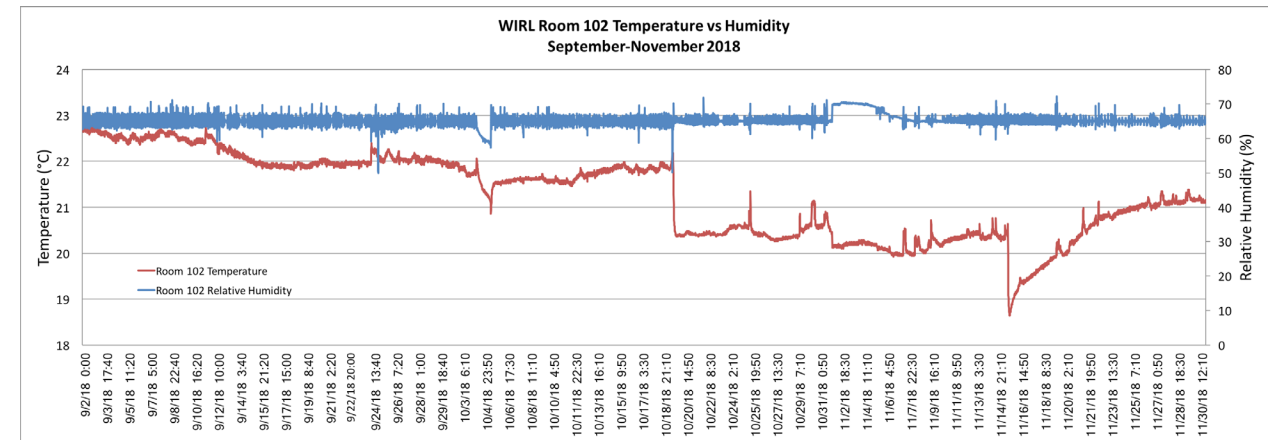


Figure 22. WIRL room 102 temperature and relative humidity readings for the period of Sept. 2 to Nov. 30, 2018.

From the data recorded by the sensors in configuration W04 and W05, we can see a consistent pattern of temperature recordings between the three sensors located above the slab insulation and the three located below. While the temperature in the conditioning room (room 102) is set to maintain 20 degrees Celsius, we can see the effects that the exterior temperature plays on the sensors located below the slab as the ground cools and pulls heat away from the building. We see the effects of this on the values recorded by the sensors as there is a general downward trend in the reported values between the dates of July 19 2018 and Jan. 12, 2019 of approximately 2C as the exterior air temperature and ground temperature decrease.

We can see that two large discrepancies exist in the W04 and W05 sensor data on Oct. 19 and Nov. 15, 2018. These are found to correlate with the temperature records which were recorded in the room over the same period (Figure 22). Due to the room's use for storing wood and materials for testing in the lab, it is believed that these occurrences correspond to the door to the room being left open during material movement in and out of the room for research or testing purposes. The temperature drop in the room sensors occurs with a delay to the drop in temperature in the room, indicating the time delay that occurs in the cooling of the concrete slab to meet the room temperature.

The values recorded by the W04 and W05 sensor configurations show the influence that the in-floor heating system and sub-soil temperatures have on the under-slab recorded temperatures. As discussed by Rantala (2005) the influences of internal boundary temperature and the thermal resistance of the slab structure are the two most significant factors affecting the fill temperature distribution beneath the center of the slab, with the impact of the external boundary temperature (sub-soil) increasing near the external wall lines. From figures 20, 21 and 22, we can see the effect that the drops in interior temperature have on the W04 and W05 sensors. This influence is most notable in the three above-slab insulation sensors. These changes in temperature are also reflected in the three below-slab insulation sensors, however the sub-slab fill temperature is also seen to have an influence, with the sensors showing values one to two degrees colder than those located above the insulation. As noted by Rantala (2005), a thermal build-up of backfill temperatures occurs during the first year of a new building, with the temperature build-up beginning during the first heating season and the following summer. Following this build-up, a thermal balance between the slab and subsoil have been reached and further changes in fill temperature may be predicted based on changes in surrounding internal and external boundary conditions. Therefore, while the findings of the W04 and W05 sensor configurations illustrate the correlation between the slab temperature and sub-slab sensor readings, further conclusions regarding the thermal performance of the WIRL building slab will only be made following this recommended build-up time period.

## Primary Energy Demand

To calculate the primary energy (electricity) demand for the WIRL building, the estimated annual electricity use for all heating, dehumidification and cooling, domestic hot water generation and equipment usage was included in the PHPP Passive House model. The equipment energy use for the building includes not only lighting and computer operation, but the estimated annual energy use of the testing and research equipment that has been installed in the building. The use of

this equipment presented a unique challenge for modeling the primary energy demand of the building, which is restricted to 120 kWh/m2a (Passive House Institute, 2015). It was important that the values for energy consumption were accurate not only for the building certification under the Passive House program, but for sizing the furnace for the building as well, as internal heat gains from the operation of the equipment had to be considered.

In calculating a building's estimate energy demand, the PHPP software multiplies the energy demand for the relevant components by a Primary Energy (PE) factor. The PE factor is used to account for the energy content of the raw material and the losses from distribution, conversion and delivery of the selected energy type for the given component to the end-user. Based on the energy consumption of the WIRL building, the projected annual energy demand for the building was 53.9kWh/m2\*a (56,109.90kWh/a). Multiplied by the appropriate PE factors, the total estimated annual Primary Energy consumption for the building was 116.0kWh/m2\*a (Figure 23). The total treated floor area of the building used for all calculations is 1041.2m2.

Energy demand Reference: Treated floor area	Efficiency		Final energy		PER			PE		CO <sub>2</sub>	
	Calculati on	User defined value	Contribution (final energy)	Final energy demand	PER factor	Effective PER factor (including biomass contingent)	PER specific value	PE factor	PE value	CO <sub>2</sub> emissions factor (CO <sub>2</sub> -eq) kg/kWh	CO <sub>2</sub> eq emissions kg/(m <sup>2</sup> a)
	-	-		kWh/(m <sup>2</sup> a)	kWh/kWh	kWh/kWh	kWh/(m <sup>2</sup> a)	kWh/kWh	kWh/(m <sup>2</sup> a)	kg/kWh	kg/(m <sup>2</sup> a)
<b>1-PE factors (non-renewable) PHI Certification</b>											
<b>1-CO<sub>2</sub> factors GEMIS (Germany)</b>											
							<b>61.3</b>		<b>116.0</b>		<b>24.1</b>
<b>Heating</b>			100%				1.10	16.7	1.30	19.7	4.4
Electricity (HP compact unit)					1.60				2.60	0.532	
Electricity (heat pump)					1.60				2.60	0.532	
District heating: 1-None					2,8(4.5)/3.3					0.000	
Wood and other biomass					1.10				-		
Natural gas / RE gas	0.98		100%	13.1	1.75	1.10	14.4	1.10	14.4	0.250	3.3
Heating oil / RE methanol					2.30			1.10		0.320	
Solar thermal system									2.60	0.532	
Electricity (direct)		1.00			1.60				2.60	0.532	
Aux. electricity (heating, wintertime ventilation)				2.0	1.60	1.10	2.2		2.60	0.532	1.1
<b>Cooling and dehumidification</b>							2.0		5.1		1.0
Electricity cooling (heat pump)	3.90			0.0	1.00			0.0	2.60	0.1	0.0
Auxiliary electricity cooling, ventilation summer				1.9	1.00		1.9		2.60	0.532	1.0
Electricity dehumidification (heat pump)					1.00				2.60	0.532	
Auxiliary electricity (dehumidification)					1.00				2.60	0.532	
<b>DHW generation</b>			100%				1.75	5.6	1.11	3.6	0.8
Electricity (HP compact unit)					1.10				2.60	0.532	
Electricity (heat pump)					1.10				2.60	0.532	
District heating: 1-None					2,8(4.5)/3.3					0.000	
Wood and other biomass					1.10				-		
Natural gas / RE gas	0.81		100%	3.2	1.75	1.75	5.6	1.10	3.5	0.250	0.8
Heating oil / Methanol					2.30			1.10		0.320	
Solar thermal system									2.60	0.532	
Electricity (direct)					1.10				2.60	0.532	
Aux. electricity (DHW + solar DHW)				0.0	1.10	1.10	0.0		2.60	0.532	0.0
<b>Household electricity</b>				33.7			1.10	37.1		87.7	17.9
Electricity (household or non-residential lighting, etc.)				33.4	1.10	1.10	36.8		2.60	0.532	17.8
Auxiliary electricity (other)				0.3	1.10	1.10	0.3		2.60	0.532	0.2
<b>Gas / RE gas dry/cook</b>				0.0	1.75		0.0		2.60	0.270	0.0

Figure 23. WIRL estimated final energy demand and Primary Energy demand (kWh/m2\*a). The Primary Energy demand (ninth column) is a sum of the final energy demand values (fourth column) multiplied by the appropriate PE factor shown in the eighth column.

The cumulative energy consumption for the WIRL building has been recorded since July 13th, 2018. The total energy consumption of the building on Feb. 28, 2019 was 65,166.36kWh of energy (Figure 24).

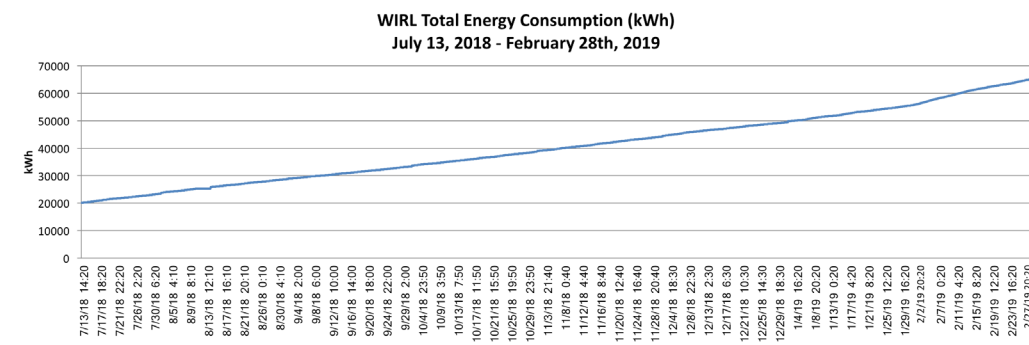


Figure 24. WIRL total cumulative energy consumption (kWh) for the period of July 13, 2018 to Feb. 28, 2019.

At the time energy consumption readings began, an initial 20,127.22kWh of energy had already been consumed. It is unknown when the actual start date for this energy consumption began, and whether it included construction work being done in the building before completion. Therefore, when calculating the average energy consumption per month, this initial energy consumption was removed.

For the period of Aug. 2018 to Feb. 2019, the average monthly energy consumption for the WIRL building was 4.22kWh/m2, (4392.63kWh) per month (Table 11). If we are to use these values to estimate the projected annual energy consumption of the building, we find the building is estimated to use 50.64kWh/m2\*a (52,711.59kWh/a). This is 3.26kWh/m2\*a (3398kWh/a) less than estimated by the PHPP model which was completed for the building.

building consumption prior monitoring (kWh)	20127.22
Month	total kWh consumption (for month)
Jul-18	3324.55
Aug-18	5281.64
Sep-18	4576.79
Oct-18	4213
Nov-18	4219
Dec-18	4213
Jan-19	4213
Feb-19	4032

Table 11. WIRL total cumulative energy consumption (kWh) for the period of July 13, 2018 to Feb. 28, 2019.

While the projected annual energy consumption based on energy use to date is less than that calculated by PHPP, we believe further data collection and analysis is required for the energy consumption of the building before a substantial comparison of the actual building performance to the PHPP model can be made. It is important to note that some of the equipment that was included in the PHPP model was only installed in the lab in February 2019. The operation of this equipment was averaged over a one-year period for the calculation of total energy consumption in the PHPP model. The actual operation of the equipment is dependent on research and testing schedules set by the faculty of the University and can vary greatly by month. Therefore, the actual energy use values should only be compared once a complete one-year cycle of operation and use is complete. In addition, external factors such as weather can influence the energy consumption of mechanical equipment, such as the pre-heaters used for the supply air on the HRV units, increasing the energy consumption and causing discrepancies between the modeled energy consumption and actual performance. Therefore, while the current monthly energy consumption data shows a good correlation with what was estimated in the PHPP model, we do not have strong confidence in comparing the two values until all of the equipment which was included in the PHPP model has been installed and is operating in the lab for a more extensive period of time.

# Conclusion and Further Steps

The thermal performance and energy consumption of the WIRL building to date has shown good correlation with the estimates modeled in the PHPP program. The sensors that were installed in the north and south walls demonstrate good hygrothermal behavior, with no record of 100% relative humidity (saturation) occurring in the assembly. The sensors that were installed in the floor agree with previous reports regarding the heat transfer through slab-on-grade systems and demonstrate the impact that small changes in substrate temperature can have. It is believed that the completion of data collection over a one-year cycle will provide further evidence to the annual performance of the assemblies and a more accurate comparison between their actual performance and the values presented by the PHPP model.

The monthly fuel consumption of the building supports the thermal performance and thermal energy consumption estimates made by the PHPP model. Discrepancies between the modeled thermal energy (natural gas) consumption of the building and the actual consumption correlate strongly with discrepancies between the design heat loss temperatures used by the software and the actual temperature profiles for each month.

The completion of a second air leakage test on the building demonstrated that the building still maintains a sufficiently low air change rate and meets the Passive House certification standard requirement. Leakage points found during testing demonstrated the effect the operation of the overhead bay door had, as well as the use of the exterior doors to the building. All were found to have leakage around them during testing and illustrate the importance of regular maintenance on seals and hardware to maintain a tight air-seal.

Current energy consumption values show a strong correlation with the PHPP model. However, it is believed that no substantial claim on the final energy consumption of the building can be made at this time due to the inconsistent operation of testing equipment. Further conclusions and discussion may be made following the completion of a full one-year data collection period.

Following the completion of the collection and analysis of the performance data for the UNBC WIRL building over the given reporting period, the following recommendations can be made:

- During the collection and analysis of data from the sensors installed in the north and south wall it was discovered that several of the sensor configurations had malfunctioned and were not transmitting data. Moving forward, it is recommended that an attempt be made to repair or replace these sensors where possible to allow for continued data collection.
- Further analysis of the hygrothermal performance of the north and south wall assemblies may be made if temperature and humidity sensors were installed on the interior and exterior side of the assemblies, including specific thermal transmittance values (u-value) and seasonal condensation probabilities (Glaser diagram). This will allow for a greater analysis of the performance variations that occur for different exposures on the building.
- Monitoring of the floor slab performance should continue so that the long-term performance and possibility of building slab and subsoil thermal balance may be observed should it occur.
- A detailed review of all equipment installed in the building that uses electrical energy should be performed. It may benefit the analysis of the collected data if individual sensors were installed on equipment that is not separated from the main energy consumption data collection, such as employee computers. This may give researchers a better idea of where electrical energy is being consumed and compare it to what was estimated in the final PHPP model.

# Acknowledgements

This research was funded by Forestry Innovation Investment Ltd. The authors thank UNBC's Facilities Management team for providing information and support throughout the data collection and analysis that was used in the writing of this case study. Special thanks to Phil Maxam, Ryan Stern and Michael Billups (UNBC) for assisting in the collection and analysis of the sensor data.

# References

Government of British Columbia. (2018). *CleanBC*. Victoria: Government of British Columbia.

Government of Canada. (2019). *Hourly Data Report*. Retrieved from Government of Canada: [http://climate.weather.gc.ca/climate\\_data/hourly\\_data\\_e.html?hlyRange=2009-10-08%7C2019-03-23&dlyRange=2009-10-22%7C2019-03-23&mlyRange=%7C&StationID=48370&Prov=BC&urlExtension=\\_e.html&searchType=stnName&optLimit=yearRange&StartYear=1840&EndYear=2019&selR](http://climate.weather.gc.ca/climate_data/hourly_data_e.html?hlyRange=2009-10-08%7C2019-03-23&dlyRange=2009-10-22%7C2019-03-23&mlyRange=%7C&StationID=48370&Prov=BC&urlExtension=_e.html&searchType=stnName&optLimit=yearRange&StartYear=1840&EndYear=2019&selR)

National Energy Board. (2017). *Canada's Energy Future 2017 - Supply and Demand Projections to 2040*. Ottawa: Government of Canada.

Natural Resources Canada. (2013). *Energy Efficiency Trends in Canada*. Ottawa: Government of Canada.  
Passive House Institute. (2015). *Passive House Institute/About Us*. Retrieved 03 12, 2019, from Passive House Institute: [https://passivehouse.com/01\\_passivehouseinstitute/01\\_passivehouseinstitute.htm](https://passivehouse.com/01_passivehouseinstitute/01_passivehouseinstitute.htm)

Passive House Institute. (2015). *Passive House Requirements*. Retrieved from Passive House Institute: [http://www.passiv.de/en/02\\_informations/02\\_passive-house-requirements/02\\_passive-house-requirements.htm](http://www.passiv.de/en/02_informations/02_passive-house-requirements/02_passive-house-requirements.htm)

Province of British Columbia. (2015). *Understanding B.C.'s Building Regulatory System*. Victoria: Office of Housing and Construction Standards.

Rantala, J. (2005). *On Thermal Interaction between Slab-on-Ground Structures and Subsoil in Finland*. Tampere: Tampere University of Technology.

U.S. Department of Energy. (2019). *Air Sealing for New Home Construction*. Retrieved from Energy.gov: <https://www.energy.gov/energysaver/air-sealing-your-home/air-sealing-new-home-construction>



**UNBC** UNIVERSITY OF  
NORTHERN BRITISH COLUMBIA  
**Wood Innovation  
Research Laboratory**